

Pluronic F127 Hydrogel Characterization and Biofabrication in Cellularized Constructs for Tissue Engineering Applications

*Original*

Pluronic F127 Hydrogel Characterization and Biofabrication in Cellularized Constructs for Tissue Engineering Applications / Gioffredi, Emilia; Boffito, Monica; Calzone, Stefano; Giannitelli, Sara Maria; Rainer, Alberto; Trombetta, Marcella; Mozetic, Pamela; Chiono, Valeria. - 49:(2016), pp. 125-132. ( The Second CIRP Conference on Biomanufacturing Manchester 29-31 July 2015) [10.1016/j.procir.2015.11.001].

*Availability:*

This version is available at: 11583/2656808 since: 2016-11-22T18:41:53Z

*Publisher:*

Elsevier

*Published*

DOI:10.1016/j.procir.2015.11.001

*Terms of use:*

This article is made available under terms and conditions as specified in the corresponding bibliographic description in the repository

*Publisher copyright*

(Article begins on next page)

The Second CIRP Conference on Biomanufacturing

## Pluronic F127 hydrogel characterization and biofabrication in cellularized constructs for tissue engineering applications.

Emilia Gioffredi<sup>a</sup>, Monica Boffito<sup>a</sup>, Stefano Calzone<sup>a</sup>, Sara Maria Giannitelli<sup>b</sup>, Alberto Rainer<sup>b</sup>,  
Marcella Trombetta<sup>b</sup>, Pamela Mozetic<sup>b</sup>, Valeria Chiono<sup>a\*</sup>

<sup>a</sup>Politecnico di Torino, Department of Mechanical and Aerospace Engineering, Corso Duca degli Abruzzi 24, 10129 Turin, Italy

<sup>b</sup>Universita Campus Bio-medico di Roma, Tissue Engineering Lab, Via Alvaro del Portillo 21, 00128 Rome, Italy

\* Corresponding author. Tel.: +39 011 0906920; fax: +39 011 0906999. E-mail address: [valeria.chiono@polito.it](mailto:valeria.chiono@polito.it)

A new method for printing cellularized scaffolds from thermosensitive hydrogels was here proposed. Pluronic F127 solutions and hydrogels in water-based media (15–40 %w/v) were investigated by rheological analysis and tube inverting test. Pluronic F127 hydrogel with 25%w/v concentration was selected as bioink due to its fast gelation at 37°C (5 min), suitable viscoelastic properties ( $G' = 16500$  Pa at 37°C), pseudoplastic behaviour and fast viscosity recovery after shearing (approximately 5 s). Not cellularized and cellularized (with Balb/3T3 fibroblasts) scaffolds with a 0°/90° pattern were fabricated by additive manufacturing technique. Cells were well distributed along scaffold filaments and cell viability was preserved during printing.

© 2015 The Authors. Published by Elsevier B.V. This is an open access article under the CC BY-NC-ND license (<http://creativecommons.org/licenses/by-nc-nd/4.0/>).

Peer-review under responsibility of the scientific committee of The Second CIRP Conference on Biomanufacturing

**Keywords:** Pluronic F127; rheology; bioprinting; hydrogels; gelation.

### 1. Introduction

Hydrogels are three-dimensional (3D) hydrophilic polymeric networks able to retain large amounts of water or biological fluids, and characterized by soft and rubbery consistency in analogy to living tissues [1,2]. Additional advantages of hydrogels are related to the possibility to include biomolecules such as growth factors within the hydrogel network for controlled release [3] as well as the ability of a few types of hydrogels to be used as injectable systems for cell therapy or drug delivery [3–5]. Depending on the mechanism of gel formation, hydrogels can be classified as: (i) chemical (or permanent) gels if the sol-to-gel transition involves the formation of a chemically crosslinked polymeric network [5,6] and (ii) physical (or reversible) gels if the gel forms through non covalent interactions between the chains. In the case of stimuli-sensitive physical gels, the sol-to-gel transition is triggered by changes in temperature (thermo-sensitive hydrogels), pH (pH-sensitive hydrogels) or analyte concentration (analyte-sensitive hydrogels) [7]. In particular, thermo-sensitive hydrogels are interesting in biomedical applications, since temperature control can be easily achieved [8–10]. Two different types of thermo-sensitive hydrogels exist

that undergo gelation either by cooling below the upper critical gelation temperature (UCGT) or by heating above the lower critical gelation temperature (LCGT), respectively. Hydrogels with LCGT behavior and sol-to-gel transition at 37°C have gained increasing attention in the biomedical field as carriers for cells, drugs and biomolecules, since they allow encapsulation in mild conditions (temperature  $\leq 37^\circ\text{C}$ ). Such hydrogels can be easily injected *in situ* in the sol state and undergo gelation at body temperature, thus allowing the complete filling of body cavities and defects before gelation.

In the last decade, both chemical and physical hydrogels have been successfully employed as scaffold-forming materials for cell printing technology [11]. Cell printing is a computer-aided tissue engineering technology based on the layered deposition of cellularized hydrogels to form complex 3D constructs [11–13]. In this work, a new approach was developed for cell printing using thermo-sensitive hydrogels. The proposed method was based on the following sequential steps: (i) the cells were first dispersed into a polymeric solution; (ii) the mixture was poured into the dispenser of an additive-manufacturing printer; (iii) sol-to-gel transition was induced by heating the dispenser to 37°C with the aim to avoid cell sedimentation; (iv) finally, a cellularized scaffold was extruded

layer-by-layer on a thermostated plate at 37°C, according to a computer-driven design.

Pluronics or Poloxamers are non-toxic FDA approved poly(ethylene oxide)/poly(propylene oxide)/poly(ethylene oxide) (PEO-PPO-PEO) triblock copolymers, which aqueous solutions undergo sol-to-gel transition with increasing the temperature above a LCGT. A variety of Pluronics is available on the market, differing for the molecular weight of the building blocks and the ratio between hydrophobic and hydrophilic units. Therefore, Pluronics allow the preparation of thermosensitive hydrogels with different properties, e.g. in terms of critical gelation concentration (CGC) and gelation time at physiological conditions. Pluronic F127 (F127) gels have been widely investigated in the literature as cell and drug carriers thanks to their low toxicity, reverse thermal gelation, high drug loading capabilities and ability to gel in physiological conditions at relatively low concentrations [14-18]. In addition, they have also been studied for cell printing applications since they are biologically inert towards multiple cell types, gel between 10 and 40°C (depending on the concentration), show a broad range of viscosities and can be easily printed without excessive stress for the encapsulated cells [19-21]. Moreover, they can be easily rinsed away after printing (if desired) by simply decreasing the temperature below the LCGT. In this work, F127-based hydrogels, prepared in deionized water, phosphate buffered saline and Dulbecco's Modified Eagle Medium (with concentrations in the 18-40 % w/v range) were prepared and characterized by rheological analysis, tube inverting and gelation time tests. The aims of this characterization were: (i) to study the effects of solution concentration and solvent type on hydrogel properties, and (ii) to select an optimal F127 concentration for the preparation of cellularised scaffolds by the here developed cell printing approach through additive-manufacturing of cellularised thermosensitive hydrogels.

## 2. Materials and Methods

### 2.1. Materials

Pluronic F127 (F127,  $M_n$ : 12600 Da, 70% w/w PEO) and all solvents were purchased from Sigma-Aldrich, Italy.

### 2.2. Hydrogel sample preparation

Hydrogel samples were prepared by dissolving F127 powder at predefined concentrations (%w/v) in an aqueous medium - deionized water, phosphate buffered saline (PBS, pH 7.4) or Dulbecco's Modified Eagle Medium (DMEM) with low glucose content - at 6°C to avoid micellisation and/or gelation during solution preparation.

### 2.3. Rheological characterization

Rheological tests on F127 solutions in deionized water, PBS or DMEM were performed by using a stress-controlled rheometer (MCR302, Anton Paar GmbH), equipped with 25

mm parallel plates. For temperature control, a Peltier system was employed.

The viscous properties of sol phase were studied at constant temperature by means of flow curves (0°C, shear rate from 1 to 100 s<sup>-1</sup>). Gel viscosity was estimated by using the same procedure, at 37°C, while the yield stress of the gels was calculated by extrapolation of flow curves at zero shear rate. Samples were poured on the rheometer lower plate at 0°C, heated to 37°C in the case of gel characterization, maintained in quiescent conditions for 15 minutes to reach the thermal stability and, finally, isothermally tested.

The viscoelastic properties of the gel phase were investigated by means of frequency sweep tests in Small Amplitude Oscillatory Shear (SAOS) conditions (frequency range from 0.1 to 100 rad/s, strain=0.1%, 37°C). The morphology and the entanglement spacing were evaluated from the linear viscoelastic response, using the frequency dependence of the elastic modulus [22].

Gel structure recovery was investigated at 37°C by subjecting the hydrogel to 100 s<sup>-1</sup> flow for 10 s followed by 100 Pa stress for 140 s.

Finally, temperature ramp tests at different heating rates and constant shear rate were carried out to obtain information about sol-to-gel transition (temperature ranging from 0°C to 40°C and shear rate=10 s<sup>-1</sup>). Temperature ramp rates were: 1, 2.5, 5 and 10°C/min.

Flow curve tests were conducted on F127 solutions with concentrations 18, 20 and 25% w/v, while sol-to-gel transition was investigated for F127 solutions with concentrations of 15, 18, 20, 25 and 30 %w/v. Structure recovery studies were carried out for F127 solutions with a concentration of 20 and 25 % w/v.

### 2.4. Tube inverting test

Sol-gel-sol phase transition behavior of aqueous Pluronic F127 solutions was investigated using the tube inverting method [23-24].

Each solution at a given concentration ranging between 18 and 40% w/v was prepared following a previously reported protocol. A solution volume of 1.5 mL was put into a Bijoux sample container (Sigma-Aldrich, Italy) with an inner diameter of 17 mm. Each sample was subjected to a controlled temperature increase from 6°C to 80°C, at a rate of 1°C/step. Each step consisted of a 1°C temperature increase, followed by isothermal maintenance for 5 minutes and tube inversion, that allowed a visual inspection of the occurrence of phase transition. The sol and the gel were identified as "flow liquid sol" and "no flow solid gel" in 30s inspection, respectively.

### 2.5. Gelation time in physiological conditions

The gelation time of F127 solutions at physiological conditions was studied by incubation at 37°C (IKA KS-4000i control) at predefined time intervals (2, 5, 10 minutes), followed by vial inversion. In this case, conditions of sol and gel were defined as "flow liquid sol" and "no flow solid gel" in 60s, respectively.

F127 solutions (1.5 mL) with concentration in the 18–40 %w/v range were prepared according to the previously described protocol and put in a Bijoux sample container (Sigma-Aldrich, Italy) with an inner diameter of 17 mm.

### 2.6. Biofabrication of Pluronic F127 hydrogel scaffolds

Porous Pluronic scaffolds were fabricated using a custom-designed additive manufacturing (AM) equipment [25], consisting of a heated dispensing head terminating with a nozzle, an X–Y motorized stage for the positioning of the dispensing head, and a z-axis for controlling its distance from the stage. The extrusion process was performed by pressure-assisted dispensing, feeding pressurized argon gas by means of a pressure line connected to a control electrovalve. Generation of the process tool-path was performed starting from a computer-aided design input geometry using a dedicated software interface.

A proper amount of Pluronic solution (25 %w/v in culture medium) was loaded into a 5 mL gel dispensing syringe (Nordson, Westlake, OH) at 4 °C. The syringe was then brought to 37 °C, leading to gelation. The hydrogel was extruded in the gel state through a 200 µm nozzle at a pressure of 1.2 bar. Squared scaffolds with a lattice homogeneous fiber spacing were obtained by depositing layers of fibers laminated in a 0°/90° pattern. The produced scaffolds were characterized by scanning electron microscopy (SEM, LEO Supra 1535).

### 2.7. Biofabrication of cellularised Pluronic F127 hydrogel scaffolds

Cellularized scaffolds were also obtained by encapsulating cells within the biomaterial. A schematic illustration of the cell-dispensing process has been reported in Figure 1. Mouse embryonic fibroblasts (Balb/3T3 cell line) were grown to a confluent monolayer, trypsinized and sedimented into a compact pellet by centrifugation. The pellet was homogeneously mixed with the ice-cold Pluronic solution at a final concentration of  $1 \times 10^6$  cells/mL. To minimize the risk of scaffold contamination during the deposition, the AM equipment was placed in a biological safety cabinet and all the materials in direct contact with cells were autoclaved before processing. The hydrogel-cell mixture was extruded into a sterile Petri dish according to the previously described printing conditions. The obtained constructs were assessed in terms of cell viability and distribution.

Cell viability was determined by MTT assay (Sigma-Aldrich, St Louis, MO, USA) which is based on the reduction of tetrazolium salts by metabolically active cells. Briefly, 3-(4,5-dimethylthiazolyl-2)-2,5-diphenyltetrazolium bromide was added to each well to a final concentration of 0.5mg/mL. After incubation for 4 h at 37 °C, 5% CO<sub>2</sub>, medium was removed and the resulting intracellular purple formazan salts were solubilized in dimethyl sulfoxide (200 µL per well). Absorbance was measured at 590 nm on a microplate reader (Tecan Infinite M200, Mannerdorf, Switzerland).

To assess cell distribution within the scaffolds, cells were previously labelled with green-fluorescent 5-chloromethylfluorescein diacetate (Cell Tracker Green CMFDA, Molecular Probes), at a final concentration of 10 µM,

and constructs were observed under an inverted fluorescence microscope.

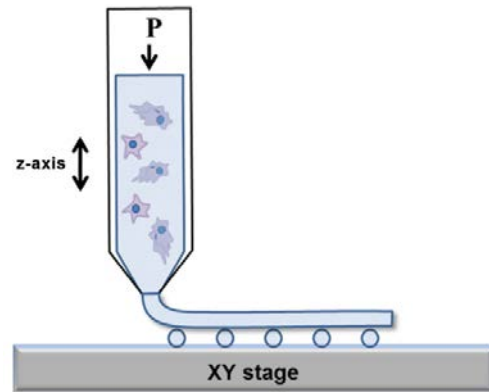


Figure 1: Schematic illustration of the fabrication process for the obtaining of cell-laden Pluronic constructs.

## 3. Results and discussion

### 3.1. Rheological characterization of Pluronic F127 hydrogels in the sol- and gel-state

Rheological tests were performed on F127 solutions and hydrogels in deionized water, PBS and DMEM to study the effect of different solvents on their sol, viscous and viscoelastic properties.

#### Flow curves

F127 solutions showed a typical Newtonian-fluid behavior and the viscosity was independent on shear rate. On the other hand, the F127 hydrogel was characterized by a power-law decrease of viscosity as a function of shear rate. As an example, the flow curves of F127 25%w/v in PBS, in both sol and gel phases (i.e. at different temperatures), are plotted in Figure 2.

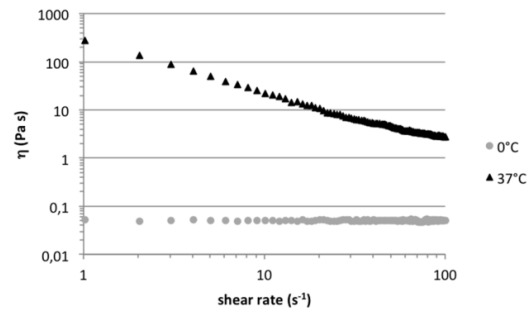


Figure 2. Viscosity of sol (0°C) and gel (37°C) phases of F127 25%w/v in PBS.

Viscosity and yield stress calculated from the flow curves of the F127 samples with 18 and 20%w/v concentration in PBS and DMEM are collected in Table 1.

Table 1. Viscosity and yield stress of F127 samples in different solvents.

	PBS		DMEM	
	18%w/v	20%w/v	18%w/v	20%w/v
Sol mean viscosity at 0°C (Pa s)	0.030	0.034	0.028	0.031
Gel viscosity at 1 s <sup>-1</sup> and 37°C (Pa s)	122	244	130	240
Yield stress at 37°C (Pa)	173	240	146	281

\*calculated from shear stress at zero shear rate.

No significant differences in viscosity and yield stress were observed for F127 hydrogels with the same concentration, prepared in PBS and DMEM. On the other hand, a 2% w/v increase of F127 concentration did not affect sol phase viscosity, whereas it markedly increased gel phase viscosity and yield stress. Hence, F127 concentration was the crucial parameter to prepare hydrogels with proper injectability properties.

Viscoelastic properties

Figure 3 reports the frequency sweep test curve of F127 25% w/v in PBS, as exemplary of the viscoelastic behaviour of F127 hydrogels. The typical gel phase exhibited G' values higher than G'' and independent on the frequency values, whereas the complex viscosity was power low-dependent.

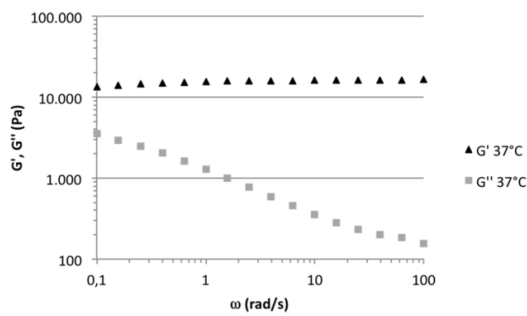


Figure 3. Viscoelastic properties of F127 25% w/v in PBS: storage (G') and loss (G'') moduli.

F127 hydrogels behaved as viscoelastic solids and their linear viscoelastic response was constant even at the lowest frequencies. The independent behavior of G' modulus on frequency suggested that the chains should disentangle before undergoing relaxation in response to additional stresses. Disentanglement is related to the length scale of the entanglement spacing (a) and the (average) monomer size (b) through the Doi and Edwards equation [26].

As an example, the G' plateau value and Doi and Edwards parameters for F127 gel with 25% w/v concentration in PBS are reported in Table 2 at three different temperatures.

Results confirmed the compact structure of F127 gels and its weak dependence on the temperature. As the monomer size (b) was constant, the entanglement spacing increased as a function of temperature.

Table 2. G' plateau value and Doi and Edwards parameters of F127 gel with 25 % w/v concentration in PBS at different temperatures.

Temperature (°C)	G' plateau (Pa)	(a <sup>2</sup> )b (nm <sup>3</sup> )
37	16500	259.27
40	15900	271.66
45	15000	292.56

Gel stability after ejection

Figure 4 shows the viscosity behavior of the F127 25 % w/v gel in PBS, after applying a step shear rate.

The structure recovery was fast: in 5 s, 100 kPa-s viscosity was reached and, in approximately 20 s, the plateau viscosity value was obtained.

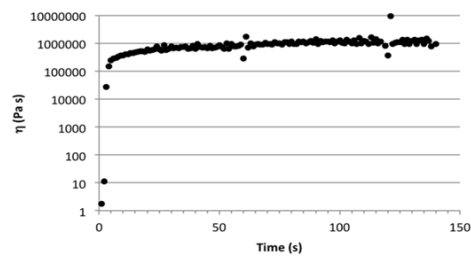


Figure 4. Viscosity recovery of F127 25 % w/v gel in PBS as a function of time at 37°C after the application of a 100 Pa stress.

3.2. Tube inverting test

Tube-inverting test was carried out on F127 solutions in deionized water, PBS and DMEM to study the effect of different solvents and solution concentration on the temperatures of phase transition.

Figure 5 reports the phase diagram of F127, while the values of LCGT and UCGT at the tested concentrations are reported in Table 3.

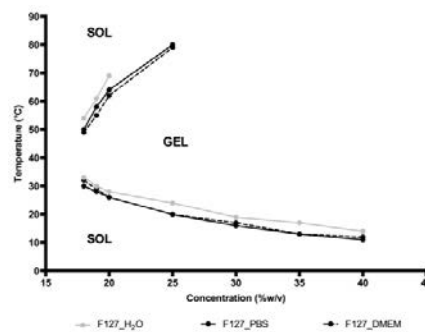


Figure 5. Sol-gel-sol phase diagram for Pluronic F127-based systems in different solvents (deionized water, PBS and DMEM with low glucose).

Table 3. LCGT and UCGT values for Pluronic F127-based hydrogels in different solvents (deionized water, PBS and DMEM with low glucose).

Concentration (%w/v)	H <sub>2</sub> O		PBS		DMEM	
	LCGT (°C)	UCGT (°C)	LCGT (°C)	UCGT (°C)	LCGT (°C)	UCGT (°C)
16	-	-	-	-	-	-
17	-	-	-	-	-	-
18	33	54	30	50	32	49
19	30	61	28	58	29	55
20	28	69	26	64	26	62
25	24	(a)	20	80	20	79
30	19	(a)	16	(a)	17	(a)
35	17	(a)	13	(a)	13	(a)
40	14	(a)	11	(a)	12	(a)

(a) UCGT is higher than 80°C

LCGT and UCGT of Pluronic F127-based hydrogels with the same concentration prepared in different solvents were approximately similar. However, LCGT for samples prepared in PBS or DMEM was slightly lower than for the samples prepared in water: this behavior was due to the salts present in PBS and DMEM that caused a "salting out" effect, i.e. a reduction of the solubility of the polymer in aqueous solution [27]. However, although the composition of DMEM and PBS is different, the "salting out" effect of the corresponding hydrogels was approximately the same.

3.3. Rheological characterization of sol-to-gel transition

Information about the sol-gel transition kinetics of F127 solutions in different solvents was obtained by means of temperature ramp tests at constant shear and different heating rates. The behavior of viscosity as a function of temperature during sol-gel transition (which is a first order transition) is depicted in Figure 6.

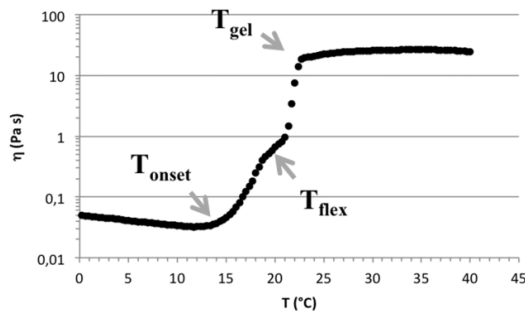


Figure 6. Viscosity of F127 25% w/v gel in PBS versus temperature at 1°C/min heating rate and 10 s<sup>-1</sup> shear rate.

The behavior of viscosity versus temperature was analyzed during heating. Initially, the viscosity decreased as a function of temperature, as typical of fluid systems (sol phase). A minimum value of viscosity was reached, followed by a monotonic increase in viscosity, due to micelle nucleation. Then, viscosity sharply increased as a function of temperature

during the growth of micelles with the conversion of the homogeneous fluid into a biphasic system. Finally, viscosity reached a plateau value and the gelation process was completed. The plateau viscosity value was 1000 times higher than for the sol phase.

Three characteristic temperatures were derived from the viscosity curves (Figure 6):

- the gelation onset temperature (T<sub>onset</sub>) at the minimum value of sol viscosity;
- the inflection temperature (T<sub>flex</sub>) at the curve flex;
- the gelation temperature (T<sub>gel</sub>) at 95% viscosity plateau value.

Sol-gel transition temperatures for different F127 concentrations in PBS and DMEM solvents are reported in the Appendix. The characteristic temperatures and their corresponding viscosities were approximately independent on the solvent. At the same solution concentration, the micelle nucleation occurred when a minimum of viscosity was reached (independently on the heating rate). The effect of the heating rate increase was an increase of the sol-gel transition temperature: a fast heating rate produced a temperature gradient within the sample (in the central portion of the material, the temperature was lower and the viscosity was higher) hence an overheating of the solution was required to reach the minimum value of viscosity.

On the other hand, at the same heating rate, all F127 solutions (except the one with 15% w/v concentration which developed a very weak gel) formed strong and stable gels, with 1000 times higher viscosity than the one of the corresponding sol phase. Finally, by increasing F127 concentration in the solvent, a decrease of the characteristic temperatures was detected, in agreement with the tube inverting test results.

A comparison between the results from the tube inverting test and rheological analysis is reported in Table 4. Data deriving from both characterizations were in agreement: some small differences were probably due to the different test conditions (tube inverting test is performed in quiescent state, while rheological analysis is performed under deformation).

Table 4. LCGT\* and T<sub>gel</sub>\*\* for F127-based hydrogels in different solvents.

Concentration (%w/v)	PBS		DMEM	
	LCGT (°C)	T <sub>gel</sub> (°C)	LCGT (°C)	T <sub>gel</sub> (°C)
15***	-	29.8	-	28.4
18	30	29.2	-	30.7
20	26	25.1	26	26.3
25	20	22.8	20	19.8
30	16	17.1	17	15.9

\*see Table 3

\*\*at 1°C/min

\*\*\*weak and not stable gel

3.4. Gelation time in physiological conditions

Gelation time at 37°C of F127 solutions prepared in deionized water, PBS and DMEM with concentrations in the 18-40 % w/v range was also studied. For applications in bioprinting technology, hydrogel gelation inside the dispenser

should be fast enough to avoid cell sedimentation. In addition, for cell printing purposes, polymer concentration in the hydrogel should be as low as possible both to minimize shear stresses to the cells during printing, and to allow nutrient and oxygen supply and waste removal [28]. All the analysed samples underwent gelation within 10 minutes. Gelation time increased with decreasing solution concentration: 2 minutes were required for the complete gelation of F127 solutions with 35 and 40 %w/v concentration, while F127 solutions with 25 and 30 %w/v concentration gelled in 5 minutes. Finally, F127 with 18, 19 and 20 %w/v concentrations showed a complete gelation after 10 minutes incubation at 37 °C. Solvent selection (deionized water, PBS or DMEM) did not influence gelation time at physiological conditions.

These findings, combined with the viscoelastic properties, the gel morphology data and the viscosity recovery analysis after shearing, indicated that F127 hydrogel with 25%w/v in PBS (or DMEM) was a promising formulation for additive manufacturing applications.

### 3.5. Pluronic F127 hydrogel biofabrication

Representative micrographs of a four-layered AM scaffold are shown in Figure 7 (A, B). The uniformity of the layered pattern, with interconnected regularly spaced pores, demonstrated the suitability of the selected gel system to be processed by the described AM technique. Results of image analysis on SEM micrographs showed agreement between the computer-generated geometry and the obtained scaffolds. The accuracy of the microfabrication technique, calculated as percentage of the fibre diameter respect to the needle size, was  $94.35 \pm 2.78\%$  ( $n=5$ ). The reproducibility of the scaffold geometry was calculated to be  $95.58 \pm 1.59\%$ , by comparing the morphological features of a significant number of scaffolds ( $n=5$ ). Furthermore, although partial fusion between the layers was often observed in hydrogel processing, fibre with circular profile were obtained through the proposed printing method. Micrographs representing a transversal section of the fabricated scaffold are presented in Figure 7 (C, D) (fibre circularity:  $0.9986 \pm 0.0011$ ).

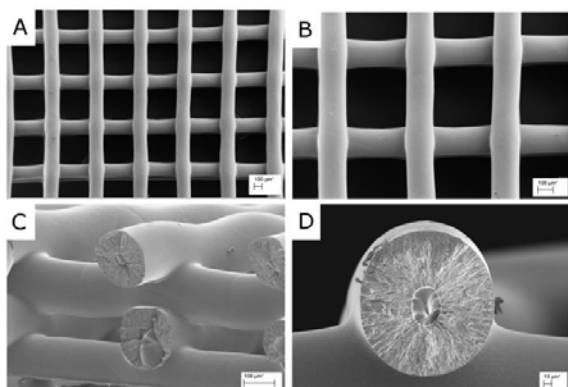


Figure 7. A,B) FEG-SEM micrographs of a four-layered hydrogel scaffold (needle  $\varnothing$  200  $\mu\text{m}$ , fiber spacing 600  $\mu\text{m}$ ); C,D) transversal sections of the fabricated fibers.

In the design of viable cell-laden structures, survival of the printed cells and uniform cell distribution within the construct are of paramount importance. Cellularised F127 scaffolds encapsulating Balb/3T3 cells were fabricated to evaluate the potential of such thermosensitive hydrogel systems for cell encapsulation during biofabrication. As shown in Figure 8, a homogeneous cell distribution was achieved. Results of MTT assay performed immediately after printing suggested that the printing process itself did not induce cell death (cell viability was higher than 80%), and no significant drop in cell viability was obtained after prolonged printing conditions (up to 30 min permanence time of the bioink in the extrusion head).

However, F127 gels were highly unstable in culture conditions, starting to dissolve within few minutes after incubation in culture medium. Thus, long term *in vitro* studies could not be conducted to assess cell viability and proliferation after extensive culture conditions.

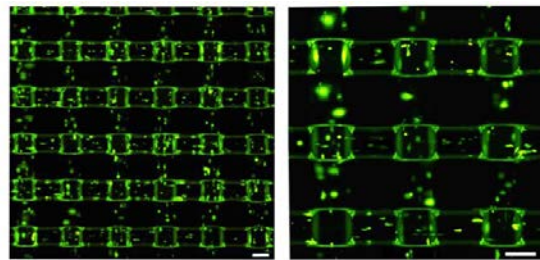


Figure 8: Encapsulation of living cells: fluorescence micrographs of cell-laden scaffolds at different magnifications. Scale bar: 200  $\mu\text{m}$ .

## 4. Conclusion

The first goal of this work was the investigation of the effect of solution concentration and solvent selection on the properties of Pluronic F127-based hydrogels. Flow curves evidenced that Pluronic F127 concentration was the crucial parameter to obtain hydrogels with proper injectability and viscoelastic properties. Solvent type only slightly influenced LCGT of the hydrogels. In detail, LCGT for samples prepared in PBS or DMEM was lower than for the corresponding samples prepared in water: this behavior was due to the salts present in PBS and DMEM that caused an effect of "salting out", i.e. a reduction in the solubility of the polymer in aqueous solution [27]. In addition, although the composition of DMEM and PBS is different, the overall salting out effect of the corresponding hydrogels was approximately the same. A good agreement between results from the tube inverting test and rheological temperature ramp analysis was observed, demonstrating that tube inverting test is a valuable analysis tool for a preliminary characterization of thermosensitive hydrogels. All the analyzed samples, with the exception of F127 15 %w/v hydrogel, showed the ability to form stable and strong gels with a viscosity about 1000 times higher than that of the corresponding sol. Further goals of this work were the development of a new approach for cell printing using thermosensitive hydrogels and the identification of the best F127 hydrogel composition (concentration and solvent type) for applications in bioprinting technology. Main requirements for the selection of the hydrogel compositions were: 1) fast

gelation at 37°C to avoid cell sedimentation in the printer dispenser; 2) low shear stresses during printing to keep cell viability; 3) suitable polymer concentration allowing fast nutrient and oxygen supply to the encapsulated cells and waste removal [28]. The F127 hydrogel with 25 % w/v concentration was selected as a promising formulation for bioprinting due to its fast gelation in physiological conditions (a volume of 1.5mL solution converted into a gel in 5 min), proper viscoelastic properties and fast viscosity recovery after shearing. Preliminary bioprinting tests showed that this hydrogel could be extruded in 3D scaffolds with a 0°/90° pattern with a high reproduction quality of the computer-aided design (CAD) file. In addition, Balb/3T3 fibroblasts showed no significant viability decrease after prolonged printing conditions (1h), proving the suitability of the adopted protocol for the fabrication of cellularised constructs. Due to their typical short residence time, high permeability and weak mechanical properties [28,29], Pluronic hydrogels are generally used in bioprinting technology as support materials to be rinsed away after printing by simply decreasing temperature below LCGT [21]. This work represents the proof-of-concept demonstration of the feasibility of a new method for cell printing using thermosensitive hydrogels. In the future, the stability of the printed hydrogel in a water environment could be increased by different routes: (i) by providing Pluronic with functional groups for chemical crosslinking during or after its gelation; (ii) by blending Pluronic with a crosslinkable polymer; (iii) by increasing its molecular weight through copolymerization; (iv) by using a different more stable thermosensitive hydrogel. These strategies will be attempted with the aim to obtain cellularised constructs by additive manufacturing, having controlled dissolution kinetics [28-31].

## Acknowledgements

FIRB 2010 Project ‘Bioartificial materials and biomimetic scaffolds for a stem cells-based therapy for myocardial regeneration’ (grant no. RBF10L0GK) financed by MIUR (Italian Ministry of Education University and Research) is acknowledged.

## Reference

- [1] Hoffman AS. Hydrogels for biomedical applications. *Adv Drug Deliv Rev* 2002;54:3-12.
- [2] Peppas NA, Bures P, Leobandung W, Ichikawa H. Hydrogels in pharmaceutical formulations. *Eur J Pharm Biopharm* 2000;50:27-46.
- [3] Gnani S, Di Blasio L, Tonda-Turo C, Macardi A, Primo L, Ciardelli G, Gambarotta G, Geuna S, Perroteau I. Gelatin based hydrogels as delivery systems for vascular endothelial growth factor release in peripheral nerve tissue engineering. *J Tissue Eng Regen Med* 2014 doi: 10.1002/term.1936.
- [4] Tonda-Turo C, Gnani S, Ruini F, Gambarotta G, Gioffredi E, Chiono V, Perroteau I, Ciardelli G. Development and characterisation of novel agar and gelatin injectable hydrogel as filler for peripheral nerve guidance channel. *J Tissue Eng Regen Med* 2014; doi: 10.1002/term.1902.
- [5] Tan H, Marra KG. Injectable, Biodegradable Hydrogels for Tissue Engineering Applications. *Materials* 2010; 3: 1746-1767
- [6] Tonda-Turo C, Cipriani E, Gnani S, Chiono V, Mattu C, Gentile P, Perroteau I, Zanetti M, Ciardelli G. Crosslinked gelatin nanofibers: preparation, characterisation and in vitro studies using glial-like cells. *Mater Sci Eng C* 2013; 33: 2723-2735.
- [7] Omidian H, Park K. Hydrogels. In: Siepmann J, Siegel R, Rathbone M, editors. *Fundamentals and Applications of Controlled Release Drug Delivery*. New York: Springer; 2012, p. 75-106.
- [8] Nguyen MK, Lee DS. Injectable biodegradable hydrogels. *Macromol Biosci* 2012;10:563-79.
- [9] Boffito M, Sirianni P, Di Rienzo AM, Chiono V. Thermosensitive block copolymer hydrogels based on poly( $\epsilon$ -caprolactone) and polyethylene glycol for biomedical applications: state of the art and future perspectives. *J Biomed Mater Res A*. 2015; 103:1276-90.
- [10] Bae SJ, Joo MK, Jeong Y, Kim SW, Lee WK, Sohn YS, Jeong B. Gelation behavior of poly(ethylene glycol) and polycaprolactone triblock and multiblock copolymer aqueous solutions. *Macromolecules* 2006;39: 4873-4879.
- [11] Imani R, Emami SH, Sharifi AM, Moshtaq PR, Baheiraei N, Fakhrazadeh H. Evaluation of novel “biopaper” for cell and organ printing application: an in vitro study. *J Diabetes Metab Disord* 2011;10:1-13.
- [12] Mironov V, Boland T, Trusk T, Forgacs G, Markwald RR. Organ printing: computer-aided jet-based 3D tissue engineering. *Trends Biotechnol* 2003;21:157-61.
- [13] Fedorovich NE, Alblas J, de Wijn JR, Hennink WE, Verbout AJ, Dhert WJ. Hydrogels as extracellular matrices for skeletal tissue engineering: state-of-the-art and novel application in organ printing. *Tissue Eng* 2007;13:1905-25.
- [14] Gilbert JC, Hadgraft J, Bye A, Brookes LG. Drug release from Pluronic F-127 gels. *Int J Pharm* 1986;32:223-8.
- [15] Yang Y, Wang JC, Zhang X, Lu WL, Zhang Q. A novel mixed micelle gel with thermo-sensitive property for the local delivery of docetaxel. *J Control Release* 2009;125:175-82.
- [16] Guzmán M, García FF, Molpeceres J, Aberturas MR. Polyoxethylene-polyoxypropylene block copolymer gels as sustained release vehicles for subcutaneous drug administration. *Int J Pharm* 1992;80:119-27.
- [17] Brunet-Maheu JM, Fernandes JC, de Lacerda CAV, Shi Q, Benderdour M, Lavigne P. Pluronic F-127 as a cell carrier for bone tissue engineering. *J Biomater Appl* 2008;24:275-87.
- [18] Khattak SF, Bhatia SR, Roberts SC. Pluronic F127 as a cell encapsulation material: utilization of membrane-stabilizing agents. *Tissue Eng* 2005;11:974-83.
- [19] Jakab K, Damon B, Neagu A, Kachurin A, Forgacs G. Three-dimensional tissue constructs built by bioprinting. *Biorheology*. 2006;43:509-13.
- [20] Kolesky DB, Truby RL, Gladman AS, Busbee TA, Homan KA, Lewis JA. 3D bioprinting of vascularized, heterogeneous cell-laden tissue constructs. *Adv Mater* 2014;26:3124-30.
- [21] Chang CC, Boland ED, Williams SK, Hoying JB. Direct-write bioprinting three-dimensional biohybrid systems for future regenerative therapies. *J Biomed Mater Res Part B: Appl Biomater* 2011;98B:160-70.
- [22] Kossut MB, Morse DC, Bates FS. Viscoelastic behaviour of cubic phases in block copolymer melts. *J Rheol* 1999;43:167-96.
- [23] Gong CY, Shi S, Dong PW, Kan B, Gou ML, Wang X, Li X, Luo F, Zhao X, Wei Y, Qian Z. Synthesis and characterization of PEG-PCLPEG thermosensitive hydrogel. *Int J Pharm* 2009;365:89-99.
- [24] Gong CY, Shi S, Dong PW, Zheng XL, Fu SZ, Guo G, Yang JL, Wei YQ, Qian ZY. In vitro drug release behaviour from a novel thermosensitive composite hydrogel based on Pluronic F127 and poly(ethylene glycol)-poly( $\epsilon$ -caprolactone)-poly(ethylene glycol) copolymer. *BMC Biotechnol* 2009;9:8-21.
- [25] Rainer A, Giannitelli SM, Accoto D, DePorcellinis S, Guglielmelli E, Trombetta M. Load-adaptive scaffold architecturing: a bioinspired approach to the design of porous additively manufactured scaffolds with optimized mechanical properties. *Ann Biomed Eng* 2012;40:966-75.
- [26] Doi M, Edwards SF. *The theory of polymer dynamics*. Oxford: Clarendon; 1988.
- [27] Pandit NK, Kisaka J. Loss of gelation ability of Pluronic F127 in the presence of some salts. *Int J Pharm* 1996;145:129-36.
- [28] Volkmer E, Leicht U, Moritz M, Schwarz C, Wiese H, Milz S, Matthias P, Schloegl W, Friess W, Goettlinger M, Augat P, Schiekier M. Poloxamer-based hydrogels hardening at body core temperature as carriers for cell based therapies: in vitro and in vivo analysis. *J Mater Sci Mater Med* 2013;24:2223-34.
- [29] Niu G, Du F, Song L, Zhang H, Yang J, Cao H, Zheng Y, Yang Z, Wang G, Yang H, Zhu S. Synthesis and characterization of reactive poloxamer 407s for biomedical applications. *J Control Release* 2009;138:49-56.
- [30] Sun KH, Sohn YS, Jeong B. Thermogelling poly(ethylene oxide)-*b*-poly(propylene oxide)-*b*-poly(ethylene oxide) disulfide multiblock copolymer as a thiol-sensitive degradable polymer. *Biomacromolecules* 2006;7:2871-7.
- [31] Cohn D, Sosnik A, Levy A. Improved reverse thermo-responsive polymeric systems. *Biomaterials* 2003; 24:3707-14.

## Appendix

Sol-gel transition characteristic temperatures of Pluronic F127 in different solvents.

	PBS					DMEM				
	$T_{\text{onset}}/\eta_{\text{onset}}$ (°C/Pa s)					$T_{\text{onset}}/\eta_{\text{onset}}$ (°C/Pa s)				
	15%w/v	18%w/v	20%w/v	25%w/v	30%w/v	15%w/v	18%w/v	20%w/v	25%w/v	30%w/v
1°C/min	16.4/0.011	14.6/0.017	13.0/0.023	12.5/0.027	8.1/0.060	15.7/0.011	14.7/0.017	13.7/0,022	10.1/0,041	7.0/0,069
2.5°C/min	16.9/0.011	15.9/0.017	14.9/0.023							
5°C/min	18.2/0.011	16.5/0.017	15.3/0.022							
10°C/min	18.5/0.011	18.4/0.016	16.8/0.021							

	PBS					DMEM				
	$T_{\text{flex}}/\eta_{\text{flex}}$ (°C/Pa s)					$T_{\text{flex}}/\eta_{\text{flex}}$ (°C/Pa s)				
	15%w/v	18%w/v	20%w/v	25%w/v	30%w/v	15%w/v	18%w/v	20%w/v	25%w/v	30%w/v
1°C/min	-	26.3/0.139	22.5/0.168	20.8/0.201	15.1/0.307	-	27.0/0.148	23.7/0.209	17.1/0.222	14.0/0.465
2.5°C/min	-	27.7/0.154	25.1/0.220							
5°C/min	-	30.3/0.182	26.6/0.270							
10°C/min	-	35.9/0.163	31.4/0.497							

	PBS					DMEM				
	$T_{\text{gel}}/\eta_{\text{gel}}$ (°C/Pa s)					$T_{\text{gel}}/\eta_{\text{gel}}$ (°C/Pa s)				
	15*%w/v	18%w/v	20%w/v	25%w/v	30%w/v	15%w/v	18%w/v	20%w/v	25%w/v	30%w/v
1°C/min	29.8/0.041	29.2/10.3	25.1/14.7	22.8/14.6	17.1/27.7	28.4/0,031	30.7/8.77	26.3/15.4	19.8/19.9	15.9/25.0
2.5°C/min	31.5/0.041	30.9/8.7	28.3/16.1							
5°C/min	34.3/0.041	33.3/9.1	29.6/16.5							
10°C/min	35.2/0.040	37.9/8.5	34.2/16.7							

\* weak gel (gel viscosity was only 4 times higher than the one of corresponding sol)